Medical Engineering and Physics 63 (2019) 57–62

Contents lists available at ScienceDirect

Medical Engineering and Physics

journal homepage: www.elsevier.com/locate/medengphy

Technical note

Robotic hip joint testing: Development and experimental protocols

Hadi EL Daou, K.C. Geoffrey Ng, Richard Van Arkel, Jonathan R.T. Jeffers, Ferdinando Rodriguez y Baena*

Department of Mechanical Engineering, Imperial College London, South Kensington Campus, London, SW7 2AZ, UK

ARTICLE INFO

Article history:
Received 12 February 2018
Revised 17 October 2018
Accepted 28 October 2018

Keywords:
Robotics
Biomechanics
In vitro
Hip
Optical tracking

ABSTRACT

The use of robotic systems combined with force sensing is emerging as the gold standard for *in vitro* biomechanical joint testing, due to the advantage of controlling all six degrees of freedom independently of one another. This paper describes a novel robotic platform and the experimental protocol used for hip joint testing. An experimental protocol implemented optical tracking and registration techniques in order to define the position of the hip joint centre of rotation (COR) in the coordinate system of the robot's end effector. The COR coordinates defined the origin of the task-related coordinate system used to control the robot, with a hybrid force/position law to simulate standard clinical tests. The axes of this frame were defined using the International Society of Biomechanics (ISB) anatomical coordinate system.

Experiments were carried out on two cadaveric hip joint specimens using the robotic testing platform and a mechanical testing rig previously developed and described by our group. Simulated internal-external and adduction/abduction laxity tests were carried out with both systems and the resulting peak range of motion (ROM) was measured. Similarities and differences were observed in these experiments, which were used to highlight some of the limitations of conventional systems and the corresponding advantages of robotics, further emphasising their added value *in vitro* testing.

1. Introduction

Advances in computer science and sensor technology have expanded the use of robots to cover new grounds in aerospace, mining, environmental monitoring, medical engineering and several other applications that require high accuracy, repeatability, manoeuvrability and flexibility. In biomechanics, robots combined with force sensors are replacing conventional systems built around instruments where one or two degrees of freedom (DOF) are controlled in displacement while the remaining DOFs are controlled using weights or passive mechanisms. Robotic systems have been shown to offer significant advantages in terms of controllability over all degrees of freedom in the task space, an ability to replay a recorded motion with high accuracy, and acquisition of synchronous readings of forces/torques and motion at high frequency rates.

Conventional *in vitro* methods incorporated universal testing machines to examine hip joint mechanics [1–3]. In addition, a hip testing rig was previously developed at Imperial College London to examine passive range of motion (ROM) and capsular restraint [4].

A robotic testing platform was developed to extensively test knee joint mechanics [5–8]. Compared to other platforms, the bespoke holders which secure the specimen inside the platform were designed to accurately reposition the joint after removing it out of the platform [8]. Robots have been widely used for cadaveric knee joint testing [9–14] and also expanded to test other joints, such as the spine [15], the shoulder [16] and, more recently, the hip [17–20]. The clear advantage of the robotic systems, equipped with force sensors, is that it can accurately control over all DOFs of the joint in force or displacement, and can apply a given force/torque and/or motion to an environment, while recording the resultant motion, forces and torques. As a result, one of the most substantial contributions the robotic platform provides is that it can accurately and precisely play back the previously recorded motion (i.e., repeating the identical pathway of motion [6]), which cannot be achieved with conventional testing setups and instruments.

To control these robotics platforms, an accurate definition of the task related coordinate system should be elaborated. This frame is then used to express the forces/moments and displacements/rotations of the tested joints. Previous studies determined the origin of this frame experimentally using a force control optimisation process where the head of the femur was pressed into the socket to find the point where only forces, not moments, were imparted by the head [21]. Other studies defined the hip joint cen-

* Corresponding author.
E-mail addresses: h.el-daou@imperial.ac.uk (H. EL Daou), f.rodriguez@imperial.ac.uk (F. Rodriguez y Baena).

https://doi.org/10.1016/j.medengphy.2018.10.006

tre using a best-fit sphere describing locations collected on the femoral head surface with the capsule intact [17]. In all these studies, the axes of this frame were defined using the ISB coordinate system [22] and aligning the frame axes with those of the Universal Force Sensor (UFS). Knowing the femoral head is naturally conchoidal and slightly aspherical in shape [23], the issue with defining the task related coordinate system would become even more problematic with any hip morphology.

The purpose of this study is to implement a new method to design and control a robotic testing platform to study hip joint biomechanics. The new method differs from those previously described in terms of the experimental protocol used to define the centre of rotation (COR) of the hip in relation to the end effector of the robot and the task-related coordinate system used to control the robot. This is complemented by the unique design of testing fixtures allowing high precision in repositioning the specimen in the platform.

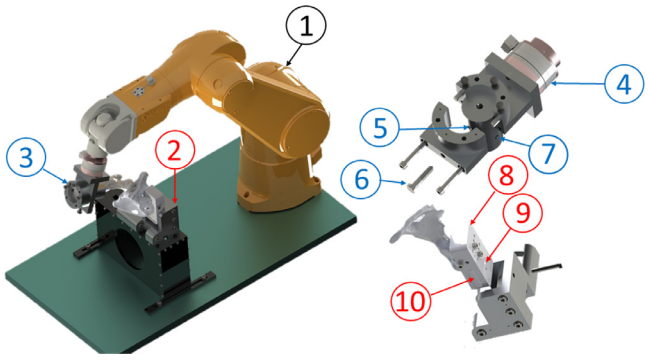

Fig. 1. Robotic testing platform composed of: 1- Staubli Tx90 Robot, 2- Bespoke Pelvic holder, 3- Bespoke Femoral holder, 4- Universal Force-moment Sensor (UFS), 5-Divot on the femoral pot, 6- Conical headed screw, 7- Femoral pot, 8-Pelvic pot, 9- Divot on pelvic pot, 10-Linear sliders on the pelvic pot.

2. Materials and methods

2.1. Hip joint preparation

Two fresh, frozen cadaveric hips ($n = 2$ males; side = left, right; age = 55, 31 years; BMI = 19, 24 kg/m^2; respectively) were used. Initially, each specimen was intact with full pelvis and femurs, then skeletonized to the hip joint capsule (i.e., removal skin, fat, muscles). Four small bone screws were placed on each hemipelvis, to serve as fiducials at specific landmarks: anterior superior iliac spine (ASIS), pubic symphysis, medial wall of the iliac crest, and posterior superior iliac spine (PSIS); for both left and right hemipelvises for each specimen (total of eight landmarks around the pelvis). The fiducials were then digitized using an optical tracking system (Optotrak Certus, Northern Digital Inc.; accuracy = 0.1 mm, resolution = 0.01 mm) and used to define the pelvis coordinate system (R_P) relative to its left and right sides. The pelvis and femur were aligned and prepared according to an established protocol that considered the International Society of Biomechanics (ISB) recommendations [22]. Each specimen was then separated into two hemi-pelvises (sectioned at the sacroiliac and pubic symphysis joints) and ipsilateral hip joint, with the proximal-third of the femur truncated at the proximal diaphysis. The femur was securely potted into a cylindrical pot, while the pelvis was potted into a custom box pot, both using polymethyl methacrylate.

After potting the hip joint, two coordinate systems attached to the femur and the pelvis were defined using the computer numerical control (CNC) machined hemispherical holes, henceforth referred as divots, on the femoral pot and the screws on the pelvis (R_F and R_P; Fig. 3). The potting protocol defined the coordinates of the axes of the ISB coordinate system on each bone in each of these frames [24]. Rigid body markers were then attached to each bone, the divots on the femoral pot and the fiducial screws were then digitised to determine the transformation matrices between the coordinate system associated with the divots and the rigid body markers on each of the bones. These two coordinate systems were used to find the transformation matrix between the robot and the passive mechanical rig setups.

2.2. Robotic testing platform

The platform comprised of a Stäubli robotic arm (TX90, Stäubli Ltd, Switzerland), a six-axis universal force-moment sensor (UFS, Omega85, ATI Industrial Automation, Apex, USA) and two bespoke holders (Fig. 1). The manipulator has six DOFs, a payload of 200 N and a repeatability of ± 0.03 mm. The UFS has a force sensing range of 3800 N in the tension/compression direction (Z-axis) and 1900 N in the other directions, with a resolution of 3/7 N in the Z axis and 2/7 N in the remaining axes. The torque sensing range is 80Nm for all axes, with a resolution of 7/748Nm in the Z axis and 5/374Nm in the other directions. The errors in repositioning the robotic platform (specimen path repeatability) were assessed in an earlier study and equal to 0.11 mm and 0.12° [8].

To securely hold the hip joint into place, one of the holders is attached to the ground and locks the pelvis pot into position. A second holder secures the femoral pot to the robotic manipulator, with a UFS is mounted in between. To allow high precision when repositioning the specimen once removed from the platform, both holders are designed to lock the bone pots in a slide fit using a screw with a conical head inserted in a cone shaped divot drilled on the surface of the pot. A similar approach was previously used to design the knee joint fixtures and was reported high precisions when repositioning specimens [8]. The pots and holders were manufactured with multiple hemispherical divots that were digitised using a four marker probe to define the pose of every element of the platform with respect to the global frame of the robot.

To define relative position of this holder with respect to the coordinate system of the robot's end effector coordinate system, a model based calibration process was used. This was carried out by moving the robot into different configurations and tracking a rigid body marker attached to its end effector using the optical tracker. The transformation between the rigid body marker and the femoral holder was found by digitising the divots on the holder and synchronously tracking the rigid body marker while the robot is held in a static position. A mathematical model was used to calculate the nominal position of the divots in the optical tracker coordinate system. A nonlinear parameter estimate solution was used to iteratively estimate the relative position of each of the divots toward the end effector's coordinate system [25]. These points defined a tool coordinate system (R_T) attached to the femoral holder.

To simulate the tests applied clinically on a hip joint, a hybrid force/position controller was used, allowing decoupled control of each of the six DOF in force or displacement. This control law required the definition of a task related coordinate system (R_C) [26]. The coordinate system used to control the robot was centred in the COR point and had its axes defined using the ISB convention [22]. The potting procedure and the femoral pot design insured that the axes of the control frame were coaxial with those of the robot's end effector and the UFS. From a control point of view, R_C was used as a virtual end effector coordinate system.

2.3. Testing protocol

The femoral pot was locked inside the robot's femoral holder and the divots on the holder and the pot were digitised to

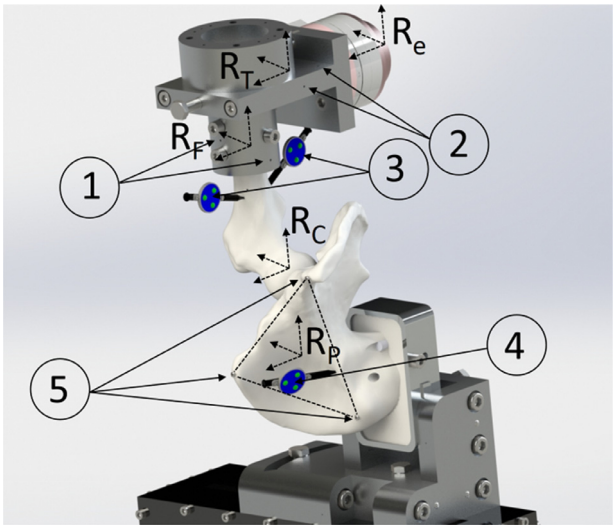

Fig. 2. Layout of different coordinates systems used for testing. 1- Divots on femoral pot, 2- Divots on femoral holder, 3- Rigid body markers on the femur, 4- Rigid body marker on the pelvis, 5- fiducial screws on the pelvis.

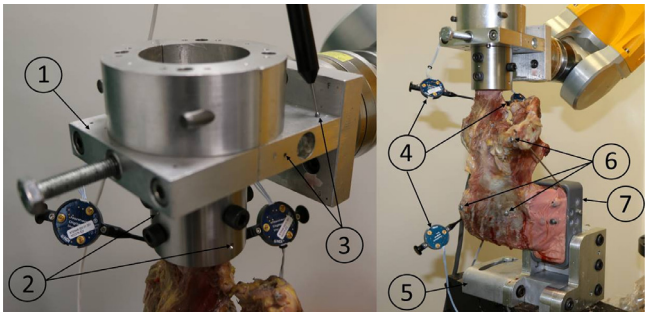

Fig. 3. Robotic testing setup. 1-Femoral holder, 2-Divots on femoral pot, 3-Divots on femoral holder, 4-Rigid body markers, 5-Pelvic holder, 6-Pelvic fiducial screws, 7-Pelvic pot.

determine the transformation between the femoral pot and the robot's end effector.

The pelvic pot was then secured inside the pelvic holder and two rigid body markers were attached to the femur (Fig. 2). With the femur held in a static position, the divots on the femoral pot were digitised and the pose of the rigid body marker was measured to determine the transformation between the coordinate system associated with the divots and that of the rigid body marker. The femur was moved manually throughout its ROM, as described by Camomilla et al. [27], whilst tracking the positions of the rigid body markers. A sphere fitting, least squares approach was used to define the coordinates of the centre of rotation of the femoral head in R_F. This also provided the coordinates of this point in the end effector coordinate system (R_e) and R_T, once the specimen was secured in the platform.

Rotation laxities were measured in response to 5-Nm AB/AD and 4-Nm IE torques respectively. The values of these torques were chosen based on similar studies to reach a maximal amplitude of motion, but not go beyond the limit that would damage the joint [17]. During the IE test, the AB/AD orientation was preserved under position control and vice-versa. One hip was used for the IE tests and the other for the AB/AD tests, as both tests were carried out on different days. The AB/AD tests were carried out at two flexion angles 30° and 90° whilst the IE ones were performed at 0° and 30° of hip flexion.

In the robotic trials, the hip was secured inside the platform at full extension. The neutral position was then found by minimising forces and moments acting across the hip at full extension using the hybrid force/position controller. The hip was driven into different flexion angles at fixed IE and AB/AD rotations while minimising forces in all directions. The CS (R_C) was used to report the translations and rotations with respect to hip anatomical axes.

2.4. Mechanical test rig

To better understand the differences from previous conventional systems, the hip joint specimens were tested first in a mechanical test rig, that was previously developed [28]. Tests were carried out first in the conventional rig because the setup of the specimen is longer than that of the robot and experiments needed to be repeated more than once for the ad/abduction tests. This rig was composed of two setups: one was attached to a dual-axis servo-hydraulic universal testing machine (model 8874, Instron Ltd, UK), equipped with a two-degrees-of-freedom (tension/torque) load-cell; and the other was a passive system, where a torque was applied using ropes and hanged weights to a wheel. To measure the static amplitude of motion in abduction/adduction, readings were recorded by eye off a large disc wheel, after a 5-Nm torque was applied from the hanging weights. To compare the measurements from the rig in the same starting position as the robot, rigid body markers were attached to the femur and the pelvis to track their motion. Fiducials on both bones were digitised in a static position to define the position of their associated frames in relation to the rigid body markers.

3. Results

3.1. IE rotations

Table 1 shows the results for IE rotations from the robot and the encoders of the testing machine for full extension and 30° flexion. The ROMs measured by the robot and the Instron for full extension and 30° were within a few degrees of each other, ($47.9° \pm 0.5°$, $44.94° \pm 0.1°$) and ($56.6° \pm 0.35°$, $55.34° \pm 0.18°$), respectively. To investigate this, the pose of the rigid body marker on the pelvis was assessed during the motion. The results (Fig. 4) showed that the x-y table of the conventional rig had a couple of degrees backlash due to the inherent tolerance stack associated with stacking linear bearings. This was not the case with the robot, as the live minimisation of forces in the x-y direction is managed by feedback from the load cell (i.e. no x-y table is required). With the mechanical test rig design, the rotations of the pelvis were not restrained, as the rigid body marker changed its orientation during the IE motion of the femur. Table 1 also shows two measurements from the conventional rig computed from the Certus readings: that of the femur from its neutral position and the relative IE rotation of the femur toward the pelvis. Differences were observed as the ROMs from both measurements for full extension and 30° were ($44.81° \pm 0.1°$, $39.3° \pm 0.01°$) and ($55.19° \pm 0.49°$, $50.28° \pm 0.14°$).

3.2. AB/AD rotations

As for the case of IE assessment, optical tracking was used to express the rotations from the robot and the rig in the same CS. In the mechanical test rig, eyeball readings were used to measure the resulting rotations. A comparison of the actual rotations recorded during ad/abduction laxity tests of the robot is provided in Table 2. The ROMs for the AB/AD tests measured by the robot, the Certus, and the visual readings at 30° and 90° were ($48.3° \pm 0.1°$, $42.1° \pm 0.54°$, $42.5° \pm 0.7°$) and ($68.9° \pm 0.14°$, $69.4° \pm 0.7°$, $65.5° \pm 0.7°$), respectively. There were similarities in the results at 90°, specifically those measured by the Certus and

Table 1
Measured rotation for internal/external laxity tests at 0° and 30°: α_1, α_2 = rotation angles under 4Nm of Internal–External rotation torque measured by the mechanical rig and the robot respectively; α_3 = Relative rotation between the femur & the pelvis measured by the Certus; α_4 = Rotation of the Intron's linear axis measured by the Certus.

Flexion Angle	Internal Torque 4 Nm		External Torque 4 Nm	
	0°	30°	0°	30°
α_1	9.56° ± 0.05°	10.82° ± 0.18°	35.38° ± 0.03°	44.52° ± 0.03°
α_2	8.60° ± 0.26°	8.34° ± 0.25°	39.30° ± 0.43°	48.25° ± 0.24°
α_3	8.07° ± 0.05°	7.84° ± 0.13°	31.23° ± 0.01°	42.44° ± 0.06°
α_4	9.30° ± 0.1°	10.93° ± 0.37°	35.51° ± 0.07°	44.26° ± 0.32°

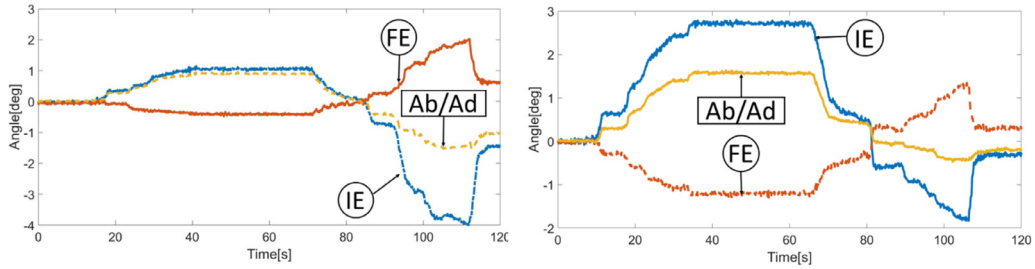

(a) **(b)**

Fig. 4. Change of orientation of the pelvic coordinates system (R_P) during an IE cycle for 0° (a) and 30° (b) of hip flexion Internal–External (IE), Flexion-Extension (FE) and Ab/adduction (Ab/Ad).

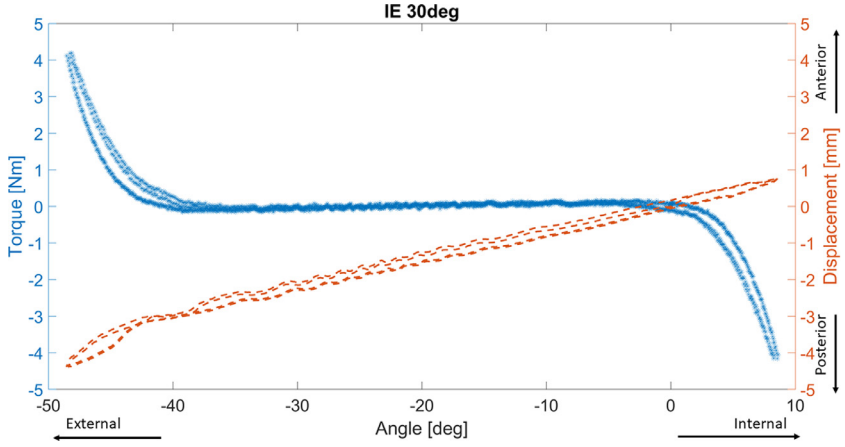

Fig. 5. Graph of IE rotations and COR anterior-posterior displacement for 4Nm IE torque applied at 30° of hip flexion using the robotic platform.

Table 2
Measured rotation for ad/abduction laxity tests at 30° and 90°: β_1, β_2, β_3 = Rotation angles under 5Nm of ad/abduction rotation torque measured with the mechanical rig (Read by eye and Certus readings) and the robot respectively.

Flexion Angle	Abduction Torque 5 Nm		Adduction Torque 5 Nm	
	30°	90°	30°	90°
β_1	29.7° ± 0.7°	37.7° ± 0°	12.8° ± 0°	27.8° ± 0.7°
β_2	29° ± 0.2°	40.2° ± 0.7°	13.1° ± 0.5°	29.2° ± 0°
β_3	33.7° ± 0.1°	40.5° ± 0.1°	14.6° ± 0°	28.4° ± 0.1°

the robot. However, an error can be observed between the eyeball and the Certus readings. This error becomes smaller at 30°, but the error between robot- and Instron-based readings becomes more important at this flexion angle.

3.3. COR translations

The robotic testing platform allowed synchronous readings of forces/torques and translations/rotations for all DOFs. This enabled us to assess secondary motion for every laxity test applied to a specimen. As such, Fig. 5 shows the translation of the COR during IE tests at 30° flexion. This graph shows that, when the femur was subjected to 4 Nm internal torque, the COR moved by 0.7 mm anteriorly while it moved posteriorly by 4.2 mm when the femur was rotated externally by a 4 Nm torque.

4. Discussion

As with any other testing method involving musculoskeletal applications (i.e., in vivo, *in silico*), there are many inherent limitations associated with *in vitro* cadaveric experiments (e.g., small sample size, tissue quality, subject-specificity or misrepresentation of a cohort, translation of data, etc.). Therefore, it is imperative to increase the accuracy and reliability of *in vitro* cadaveric testing instruments and methods, in efforts to adequately limit confounding variables, interpret the results and clinical significance. The aim of this study was to highlight the recent advancements in hip joint testing using a robotic testing platform.

Methods and experimental protocols used to develop and control a robotic platform for hip joint testing were presented. Compared to existing robotic platforms, the one described in this study has the advantage of repositioning the specimen with high precision due to the design of the specimen holders. This can permit

users to remove the specimens and allow surgeons to practice and test surgical procedures that cannot be performed when the specimen is mounted in the platform. Subsequently, the specimen can easily be repositioned. The experimental protocol also used optical tracking and registration techniques to define the position of the COR and the ISB coordinate system of each hip femur toward the robot's end effector. This COR and ISB coordinate system were used to define the task specific coordinate system used by the hybrid force/position controller.

Compared to conventional systems, the major advantages of the robotic platform were the high accuracy in applying/measuring loads and displacements in all DOFs of a joint, made possible by using force sensing and a custom-made rig to facilitate repositioning the specimens. With such a setup, human intervention was limited to securing the specimens inside the robot and running code that planned, controlled and measured the resulting forces and motion for all DOFs, with a clear improvement in experimental robustness and the accuracy and repeatability of the measurements. The 6 DOF robotic system validated by Goldsmith et al. [17] for repeatable evaluation of hip passive path and ROM clinical exams demonstrates a vast improvement in system repeatability compared to manual exam.

In addition, the robotic testing platform can track the trajectory of the hip joint at any position during internal–external, flexion-extension, abduction-adduction rotations. With the recorded motions, the robotic platform can replicate the path and permit the hip to perform the exact same motion. Combined with the ability to precisely reposition the specimen in the holders, users can first capture the path motion under load-control conditions (e.g., internal–external rotation to 4 Nm). After users remove the specimen, to perform any surgical procedures, and remount the specimens onto the holders; the robotic platform can then playback the initial recorded path of motion, in examine if there were any changes in internal–external torsional restraint [6].

To further illustrate these advantages, the experiments carried out with the robotic system were compared with an existing mechanical rig. Unsurprisingly, results showed differences and similarities in the resulting rotations. For the IE case, the robot measured a greater ROM than the conventional rig, which was expected, as the specimen was tested second in the robotic system and thus will have deteriorated slightly from the first test and the conventional rig x-y table demonstrated a backlash that had a tolerance stack that could have influenced the results. For the AB/AD case, one of the limitations of the conventional rig was the absence of measurements of the applied torque. Readings from both rigs were expressed in the same starting position using a registration technique based on optical tracking, which may have been a source of errors in measuring the internal, external, AB/AD rotations. However, such errors would not have had any effect on measuring the overall ROM during a given test.

5. Conclusion

This study introduced methods and experimental protocols to design a novel robotic testing platform to examine native hip joint biomechanics. These methods are not specific to one platform and could be applied for other platforms and joints. A registration method based on using CNC machined divots, optical tracking and robotic calibration techniques were used to define the position of a least squares estimate of the COR toward the robot's end effector and to measure its motion toward the robot and the pelvis. This COR was used as the origin of the task related coordinate system whose axes are co-axial with those of the ISB coordinate system for the femur. In comparison with an existing mechanical test rig, the robotic system demonstrated substantial improvements in terms of its ability to position the hip by minimising the forces acting on it and avoiding inherent tolerance stacking limitations with mechanical fixtures required to release degrees of freedom. Given advances in robotic technology, this data provides strong support for the implementation of robotic testing platforms in biomechanics and orthopaedics as a standard, given their superiority to traditional testing instruments and methods. We expect the new robotic testing platform to support all future hip-related studies in our laboratory.

Conflict of interest

None.

Ethical approval

This study was conducted under the terms of research ethics permit R14088-1A.

Acknowledgments

This work was funded by a grant from the EPSRC to research adverse loading of the hip joint after joint preserving and joint replacement surgery. The dual-axis Instron materials-testing-machine was provided by an equipment grant from Arthritis Research UK. The robotic test system was supported by the Wellcome Trust and EPSRC Centre of excellence for application of technology to osteoarthritis. The authors would like to acknowledge the Philip Leverhulme Trust for their kind support.

References

[1] Hewitt J, Guilak F, Glisson R, Vail TP. Regional material properties of the human hip joint capsule ligaments. J Orthopaed Res 2001;19(3):359–64.
[2] Anderson AE, Ellis BJ, Maas SA, Peters CL, Weiss JA. Validation of finite element predictions of cartilage contact pressure in the human hip joint. J Biomech Eng 2008;130(5):051008.
[3] Satpathy J, Kannan A, Owen JR, Wayne JS, Hull JR, Jiranek WA. Hip contact stress and femoral neck retroversion: a biomechanical study to evaluate implication of femoroacetabular impingement. J Hip Preserv Surg 2015;2(3):287–94.
[4] van Arkel RJ, Amis AA, Jeffers JR. The envelope of passive motion allowed by the capsular ligaments of the hip. J Biomech 2015;48(14):3803–9.
[5] Athwal KK, Daou HE, Kittl C, Davies AJ, Deehan DJ, Amis AA. The superficial medial collateral ligament is the primary medial restraint to knee laxity after cruciate-retaining or posterior-stabilised total knee arthroplasty: effects of implant type and partial release. Knee Surg Sports Traumatol Arthrosc 2016;24(8):2646–55.
[6] Kittl C, El-Daou H, Athwal KK, Gupte CM, Weiler A, Williams A, Amis AA. The role of the anterolateral structures and the ACL in controlling laxity of the intact and ACL-deficient knee. Am J Sports Med 2016;44(2):345–54.
[7] Lord BR, El-Daou H, Sabnis BM, Gupte CM, Wilson AM, Amis AA. Biomechanical comparison of graft structures in anterior cruciate ligament reconstruction. Knee Surg Sports Traumatol Arthrosc 2016:1–10.
[8] El Daou H, Lord B, Amis A, y Baena FR. Assessment of pose repeatability and specimen repositioning of a robotic joint testing platform. Med Eng Phys 2017.
[9] Woo SL-Y, Abramowitch SD, Kilger R, Liang R. Biomechanics of knee ligaments: injury, healing, and repair. J Biomech 2006;39(1):1–20.
[10] Rasmussen MT, Nitri M, Williams BT, Moulton SG, Cruz RS, Dornan GJ, Goldsmith MT, LaPrade RF. An in vitro robotic assessment of the anterolateral ligament, part 1: secondary role of the anterolateral ligament in the setting of an anterior cruciate ligament injury. Am J Sports Med 2016;44(3):585–92.
[11] Nitri M, Rasmussen MT, Williams BT, Moulton SG, Cruz RS, Dornan GJ, Goldsmith MT, LaPrade RF. An in vitro robotic assessment of the anterolateral ligament, Part 2 anterolateral ligament reconstruction combined with anterior cruciate ligament reconstruction. Am J Sports Med 2016;44(3):593–601.
[12] Noyes FR, Huser LE, Jurgensmeier D, Walsh J, Levy MS. Is an anterolateral ligament reconstruction required in ACL-reconstructed knees with associated injury to the anterolateral structures? A robotic analysis of rotational knee stability. Am J Sports Med 2017:0363546516682233.
[13] Goldsmith MT, Jansson KS, Smith SD, Engebretsen L, LaPrade RF, Wijdicks CA. Biomechanical comparison of anatomic single-and double-bundle anterior cruciate ligament reconstructions: an in vitro study. Am J Sports Med 2013;41(7):1595–604.
[14] Sasaki N, Farraro KF, Kim KE, Woo SL. Biomechanical evaluation of the quadriceps tendon autograft for anterior cruciate ligament reconstruction: a cadaveric study. Am J Sports Med 2014;42(3):723–30.
[15] Schulze M, Hartensuer R, Gehweiler D, Hölscher U, Raschke MJ, Vordemvenne T. Evaluation of a robot-assisted testing system for multisegmental spine specimens. J Biomech 2012;45(8):1457–62.

[16] Debski RE, Wong EK, Woo SLY, Sakane M, Fu FH, Warner JJ. In situ force distribution in the glenohumeral joint capsule during anterior-posterior loading. J Orthopaedic Res 1999;17(5):769–76.
[17] Goldsmith MT, Rasmussen MT, Turnbull TL, Trindade CA, LaPrade RF, Philippon MJ, Wijdicks CA. Validation of a six degree-of-freedom robotic system for hip in vitro biomechanical testing. J Biomech 2015;48(15):4093–100.
[18] Philippon MJ, Trindade CA, Goldsmith MT, Rasmussen MT, Saroki AJ, Løken S, LaPrade RF. Biomechanical assessment of hip capsular repair and reconstruction procedures using a 6 degrees of freedom robotic system. Am J Sports Med 2017:0363546517697956.
[19] Bonner Tara F, Colbrunn Robb W, Bottros John J, Mutnal Amar B, Greeson Clay B, Klika Alison K, Van Den Bogert Antonie J, Barsoum Wael K. The contribution of the acetabular labrum to hip joint stability: a quantitative analysis using a dynamic three-dimensional robot model. Journal of Biomechanical Engineering 2015;137(6):061012.
[20] Smith MV, Costic RS, Allaire R, Schilling PL, Sekiya JK. A biomechanical analysis of the soft tissue and osseous constraints of the hip joint, Knee Surgery, Sports Traumatology. Arthroscopy 2014:1–7.
[21] Colbrunn R, Bottros J, Butler R, Klika A, Bonner T, Greeson C, Van Den Bogert A, Barsoum W. Impingement and stability of total hip arthroplasty versus femoral head resurfacing using a cadaveric robotics model. Journal of Orthopaedic Research 2013;31(7):1108–15.
[22] Wu G, Siegler S, Allard P, Kirtley C, Leardini A, Rosenbaum D, Whittle M, D'Lima DD, Cristofolini L, Witte H, Schmid O, Stokes I. ISB recommendation on definitions of joint coordinate system of various joints for the reporting of human joint motion - Part I: Ankle, hip, and spine. J Biomech 2002;35(4):543–8.
[23] Menschik F. The hip joint as a conchoid shape. J Biomech 1997;30(9):971–3.
[24] van Arkel RJ, Jeffers JR. In vitro hip testing in the international society of biomechanics coordinate system. J Biomech 2016;49(16):4154–8.
[25] Sciavicco L, Siciliano B. Modelling and control of robot manipulators. Springer Science & Business Media; 2012.
[26] Raibert MH, Craig JJ. Hybrid position/force control of manipulators. J Dyn Syst Measur Control 1981;102(127):126–33.
[27] Camomilla V, Cereatti A, Vannozzi G, Cappozzo A. An optimized protocol for hip joint centre determination using the functional method. J Biomech 2006;39(6):1096–106.
[28] van Arkel RJ, Amis AA, Jeffers JR. The envelope of passive motion allowed by the capsular ligaments of the hip. J Biomech 2015;48(14):3803–9.